Generalized Classification Scheme of Toroidal and Helical Carbon Nanotubes

Chern Chuang, Yuan-Chia Fan, and Bih-Yaw Jin*

Department of Chemistry and Center of Theoretical Sciences, National Taiwan University, Taipei, Taiwan, ROC

Received October 26, 2008

In this study, we develop a generalized classification scheme for toroidal (TCNT) and helical carbon nanotubes (HCNT) containing both pentagons and heptagons simultaneously. We show that a particular class of TCNTs with n-fold rotational symmetry and well-defined latitude coordinates can be uniquely characterized by a set of four indices, and each of the indices can be linked to the relative arrangement of pentagons and heptagons in the corresponding torus. Chiral isomers or the corresponding helical derivatives, HCNTs, can also be readily derived either by introducing a chiral vector or dissecting a distorted TCNT through certain longitude. This generalized scheme can generate the whole family of fullerenes with genus one, ranging from giant TCNTs down to small ones containing only a few hundred atoms. To the best of our knowledge, almost all of the construction methods for TCNTs in the literature belong to special cases of our generalized classification scheme.

INTRODUCTION

Since the discovery of fullerene, C_{60}, by Kroto et al.,[1] followed by the discovery of carbon nanotube by Iijima,[2] a great quantity of studies of the structural and physical properties of this new kind of material was made.[3] In particular, sp^2 carbon structures containing negative curvatures with nonhexagonal defects were proposed and then observed.[4−9] Among them, toroidal carbon allotropes[11] are of special physical interests due to the potential existence of peculiar persistent currents and giant paramagnetic susceptibility in these systems.[12−19] Although experimental observation of small tori (down to 100 atoms per torus) is not yet reported, theoretical studies showed that these tori may exhibit lower cohesive energy than fullerenes and are considered as thermodynamically stable compounds.[20−26]

Systematic enumeration and construction of TCNTs as a function of carbon atoms are complicated graph-theoretical problems. Several groups had developed distinct strategies for the construction of TCNTs, which we only briefly summarize. The first systematic method was proposed by Dunlap,[27] in which he discovered the bending angle by joining two carbon nanotubes (CNT) of orthogonal chiral vectors is about 30 degrees from the original tube axis. Repeatedly connecting 6 pairs of zigzag and armchair CNTs can produce a D_{6h} torus. Itoh and Ihara's group started from a pre-existing smaller D_{nh} or D_{nd} torus.[22−25] By inserting appropriate graphitic stripes into it, a series of elongated tori is obtained. Berger and Avron developed an ingenious and tricky systematic construction rule for tiling of isosceles right-angle triangles on a rectangular plane, and such tiling can be mapped to a Clifford torus in 3-D. Given a set of 4 numbers, (m, g_1, g_m, z) in their notation, one can specify a D_{nd} torus.[20,21] Fowler et al. discovered a simple method to generate a chiral D_n isomer from a D_{nd} torus by the Stone-Wales transformation.[28,29] By choosing different positions and shapes of super cells, László et al.[37] arrived at D_{nd}-symmetric TCNTs, and, if the edges of the super cell are chosen to be intersecting the unit cell edge vectors at suitable angles, then HCNTs can be formed. In the most up-to-date classification of polygonal TCNTs of D_{6h} symmetry, Tamura et al. have found that this kind of TCNTs may possess interesting magnetic properties.[12]

Here, in this article, we show that the numerous TCNT construction and classification methods mentioned (with the exception of Dunlap's), which seem to have different features or are even totally uncorrelated, can be unified in a much more generalized scheme. Starting parent structures are those TCNTs that have well-defined latitudes, i.e. they are interconnected polyacetylene chains if viewed along certain directions with rotational symmetry. Based on these observations, we have developed a general classification and systematic construction scheme for toroidal molecules that includes, to our knowledge, almost every case in the literature. Starting from the cut-and-fold idea of Tamura et al., we further define two different structure isomerization processes that finally lead to the various stable TCNTs discussed in the literature. The correspondences of our notation to previous studies are also given in this paper. Furthermore, the HCNTs as proposed by two different groups, Akagi et al.[30] and László et al.,[37] are shown to be special cases of the current scheme. The helicities of these HCNTs can be derived directly from the parameters given in the isomerization procedure.

BASIC CONSTRUCTION SCHEME

It is well-known that inserting nonhexagons into a graphene sheet in general introduces nonzero Gaussian curvature.[9,10] Because an sp^2 carbon possesses a bond angle of approximately 120 degrees, for stability concerns, we allow only pentagons and heptagons in most parts of the current article. Polygonization of a certain surface must satisfy Euler's formula, $\chi = V - E + F$, where V, E, and F are the number of vertices, edges, and faces of the polygonization, respectively, and χ is the Euler characteristic of the

* Corresponding author e-mail: byjin@ntu.edu.tw.

10.1021/ci800395r CCC: $40.75
Published on Web 01/27/2009

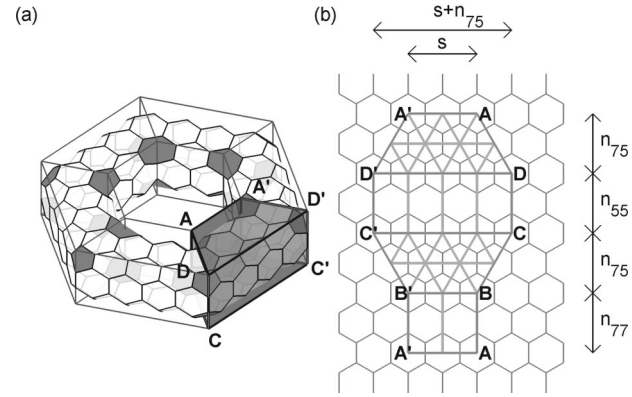

Figure 1. TCNT with indices $(n_{75}, n_{77}, n_{55}, s) = (2, 1, 1, 2)$, $(1, 0)$, and $n_{rot} = 6$. (a) The polygonal shape is depicted as skeletal frames encompassing the corresponding TCNT. The shaded region shown is a particular rotational unit cell. (b) The rotational unit cell (shaded region in (a)) is unfolded onto a planar graphene sheet. In this article we follow all the notational conventions of Tamura's group except that the symbol S_2 is replaced by s. In this and other figures of this paper, we have colored all nonhexagons, which are always located at the vertices of the polyhedron.

surface. By simple algebra, we obtain $6\chi = N_5 - N_7$, where N_5 and N_7 are the number of pentagons and heptagons, respectively. Note that the term, N_6, cancels out, which means that Euler's formula puts no constraints on the number of hexagons in the polygonization.

Achiral TCNTs. In general, the construction of a polygonal TCNT can be viewed as a cut-and-fold procedure. First, we need to cut a suitable periodic polygon with a unit cell defined in Figure 1(b) from a planar graphene sheet and then fold the remaining area to form a polygonal torus as shown in Figure 1(a). Using this technique, Tamura et al.[12] had shown that a family of achiral TCNTs with D_{nh} symmetry can be systematically constructed by polygonal prisms defined by four parameters, $(n_{75}, n_{77}, n_{55}, s)$, as given in Figure 1(b). The polygonal TCNT in Figure 1(a) has six identical rotational unit cells, and one of them is unfolded in 1(b), which consists of two rectangles and two trapezoids. Note that the rectangular patches, $ABB'A'$ and $CDD'C'$, in the unfolded periodic polygon correspond to the inner- and outer-rims of a unit cell in the polygonal torus and their corners correspond to heptagons and pentagons in the folded TCNT, respectively, whereas the two isosceles trapezoidal patches, $BCC'B'$ and $ADD'A'$, on the top and bottom of the polygonal TCNT connect both of the previous two rectangular patches. Joining six identical unit cells side-by-side, one can form a TCNT with the 6-fold rotational symmetry. The widths and heights of the two rectangles provide us four degrees of freedom to characterize each TCNT, as defined below. The parameter $s = \vec{AA'}/a$ is the width of $ABB'A'$, where a is the lattice constant of planar graphene. The width of $CDD'C'$ divided by a defines the parameter $n_{75}+s$, where $n_{75} = \vec{BC}/a$ represents the topological distance between pentagon and heptagon. The heights of the rectangular patches, $n_{77} = \vec{AB}/\sqrt{3}a$ and $n_{55} = \vec{CD}/\sqrt{3}a$, represent the topological distances between adjacent heptagons and pentagons along the vertical direction, respectively.

For convenience, we shall term TCNTs of this kind as *hollow-prism*, for geometrically they resemble a large prism structure that has a smaller coaxial prism with the same shape punched out of it. Given a hollow-prism TCNT, there are two kinds of isomerization which retain the rotational

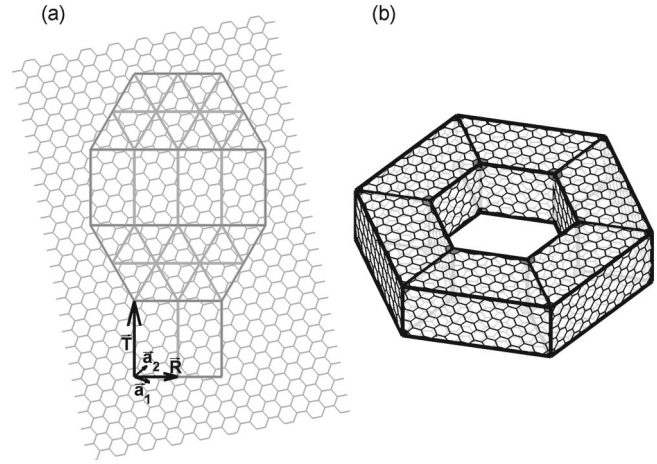

Figure 2. A chiral TCNT will be generated, if the base vector $\vec{R}$ is tilted with respect to the lattice vector a_1. We used the same indices as in 1, $(n_{75}, n_{77}, n_{55}, s) = (2, 1, 1, 2)$, but a different chiral vector $(n_1, n_2) = (2, 1)$, i.e., $\vec{R} = 2\vec{a}_1 + \vec{a}_2$, for this chiral TCNT. (a) The unfolded unit cell similar to the achiral case in 1 is shown. Depending on the chiral vector, the aspect ratio of rectangular parts is different. (b) The folded TCNT with $n_{rot} = 6$. Note that the overall polygonal shape is retained, while the zigzag pattern is tilted with respect to the skeletal frame.

symmetry. Both of them change the relative positions of the nonhexagons and, thus, tilt the original D_{nh}-symmetric structures. We shall briefly discuss how they affect the geometries of TCNTs later. The final structure of a TCNT can be obtained by optimizing the corresponding polygonal TCNT constructed with the cut-and-fold approach.

Chiral TCNTs. In this subsection, we generalize the cut-and-fold scheme to a larger family of chiral TCNTs with D_n symmetry by allowing the direction of the graphene sheet to be tilted relative to the zigzag direction. Following the usual notation of chiral CNTs, we introduce the chirality by lining up the base vector of an unfolded unit cell along a particular chiral vector, (n_1, n_2); the corresponding TCNT will belong to the D_n point group. In Figure 2 the base vector $\vec{R}$ is given by $\vec{R} = 2\vec{a}_1 + \vec{a}_2$, thus the chiral vector is $(n_1, n_2) = (2, 1)$ in this case. Similar to the achiral case discussed in the last section, we can divide the rectangular part of the unit cell into smaller, irreducible rectangular patches. So their widths are just the length of the base vector, while the height will be the shortest lattice vector, $\vec{T} = -4\vec{a}_1 + 5\vec{a}_2$, perpendicular to the base vector $\vec{R}$. In fact, this irreducible rectangular patch is exactly the unfolded unit cell of a chiral CNT with the chiral vector, (n_1, n_2).[3] Now the definitions of s and $n_{75}+s$ intuitively become the number of irreducible patches counted horizontally in these two rectangles, and n_{77} and n_{55} are the number of irreducible patches counted vertically. Note that the trapezoids as shown in Figure 2(a) can also be divided into several equilateral triangles with the base vector as their edges. Incidentally, these triangular patches are exactly the equilateral triangles in icosahedral fullerenes, as first proposed by Goldberg.[36]

With the definitions given above, we can see that the Tamura's tori correspond to the TCNTs with the chiral vector, $(n_1, n_2) = (1, 0)$, in which the irreducible rectangular and triangular patches contain a minimum number of carbon atoms, i.e. two and one atoms, respectively. Here we would like to give a brief explanation on the possible values of (n_1, n_2). The only two chiral vectors of achiral TCNTs are

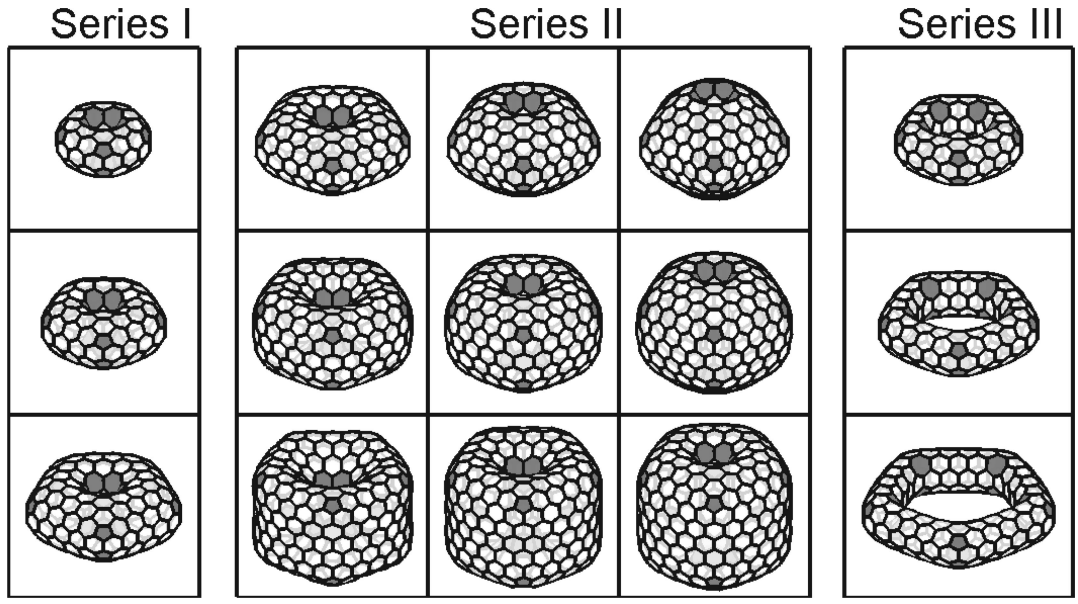

Figure 3. Three series of TCNTs are defined to show the geometric meaning of the indices. Series I, (2, 1, 1, 1) to (4, 1, 1, 1), with their n_{75} values increasing. Series II, (4, 1, 1, 1) (top left) to (4, 3, 1, 1) (top right) and (4, 1, 3, 1) (bottom left) to (4, 3, 3, 1) (bottom right). These are the two-dimensional grids of (n_{77}, n_{55}). Series III, (2, 1, 1, 2) to (2, 1, 1, 4), with their s values increasing. Chiral vector is (1, 0) and $n_{rot} = 5$.

(1, 0) and (1, 1). For chiral TCNTs, the possible values of (n_1, n_2) must satisfy $0 < n_2/n_1 < 1$ with no common divisor for n_1 and n_2, i.e. gcd (n_1, n_2) = 1.

Given these four parameters, a two-component chiral vector (n_1, n_2), and a rotational symmetry number n_{rot}, the structure of a TCNT is uniquely defined. The number of atoms N in a TCNT belonging to this type is given by

$$N = n_{rot}[2N_{rec}(n_{77}s + n_{55}(n_{75} + s)) + 2N_{tri}(2n_{75}s + n_{75}^2)] \quad (1)$$

$$N_{rec} = \frac{2(n_1^2 + n_2^2 + n_1n_2)}{\gcd(2n_1 + n_2, 2n_2 + n_1)} \quad (2)$$

$$N_{tri} = n_1^2 + n_2^2 + n_1n_2 \quad (3)$$

where N_{rec} and N_{tri} are the numbers of atoms in an irreducible rectangular and equilateral triangular patches of a rotational unit cell, respectively. The first term in the square bracket of eq 1 corresponds to the number of carbon atoms within the rectangular patches located on the inner and outer side of the hollow-prism, while the second term corresponds to the total number of atoms on the top and the bottom trapezoids.

Although n_{55} need not be equal to n_{77} in the general situation, we will concentrate on the TCNTs with $n_{77} = n_{55}$ in this article. As mentioned above, the shapes of this kind of TCNTs would look like a n_{rot}-fold symmetric prism with a smaller coaxial n_{rot}-fold symmetric prismatic hole, as shown in Figure 1(a) and Figure 2(b). All TCNTs discussed later in this paper, except where otherwise mentioned, are small achiral TCNTs with chiral vectors, (n_1, n_2) = (1, 0) and (1, 1). These two families of TCNTs have zigzag and armchair structures along the latitude direction, respectively. The total numbers of atoms for these two situations are

$$N_{zig} = n_{rot}[4(n_{77}s + n_{75} + s) + 6(2n_{75}s + n_{75})] \quad (4)$$

$$N_{arm} = n_{rot}[4(n_{77}s + n_{75} + s) + 2(2n_{75}s + n_{75})] \quad (5)$$

To clarify the geometric meaning of the indices, we introduce three series of TCNTs with D_{nh} symmetry as shown in Figure 3. Each series represents a particular evolution of TCNTs as a function of certain indices among the four parameters, (n_{75}, n_{77}, n_{55}, s). More specifically, series I corresponds to TCNTs with the increasing of n_{75} while keeping other parameters, n_{77}, n_{55}, and s, constant. Series II corresponds to varying (n_{77}, n_{55}). Interestingly, in the large N limit, the diagonal diagrams, i.e. TCNTs that satisfy the condition $n_{55} = n_{77}$, converge to the end-capped double-wall CNTs.[3,8,31] TCNTs in series III corresponding to the increasing of s are particularly important since, in the large s limit, this family of TCNTs is very similar to the carbon nanotori without 5−7 pairs which are extensively studied in the literature.[15−19]

Inner- and Outer-Rim Rotation. In addition to TCNTs belonging to the polygonal structures in Figure 2, there exists a more general class of hollow-prism TCNTs that consists of a 30-degree rotation for the central hollowed hexagonal hole by moving heptagons to suitable positions on the graphene honeycomb lattice as shown in Figure 4. Unlike structures in Figure 2, the inner- and outer-rims of the resulting polygonal structure are, in general, no longer parallel with each other. Moreover, its inner-side chiral vector is changed to the armchair conformation along the circumference, while the structure of its outer side remains in the zigzag conformation. Of course, as can be seen clearly from Figure 4, the latitude coordinates are no longer well defined after this kind of transformation. Similarly, we can also perform the rotation for the outer-rim hexagon 30 degrees on the graphite lattice; the outer-rim of the resulting structure will now have the armchair conformation. Particularly, if the parent TCNT considered is a double wall carbon nanotube (DWCNT), with both ends capped, the inner- or outer-rim rotated TCNT is like a DWCNT consisting of the coaxial armchair- and zigzag-CNTs joined at both ends.

Stability. Energetically, pentagons (heptagons) have a strong tendency to be located in the areas with positive (negative) Gaussian curvatures. Thus, by restricting the locations of pentagons to the outer-rim and those of

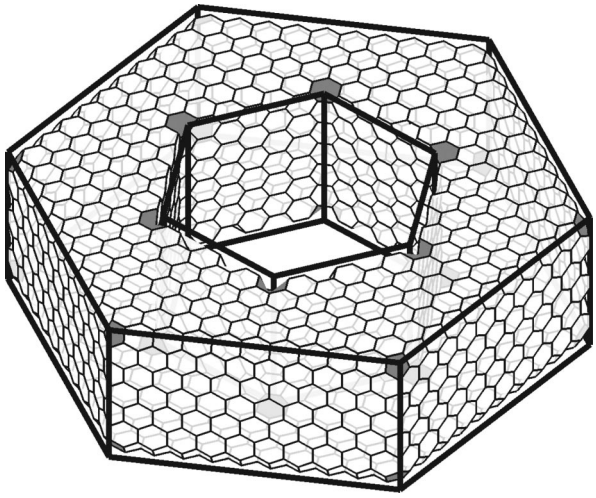

Figure 4. Another form of the hollow-prism TCNT. In this case the outer side of the prism has a horizontal zigzag pattern, and the inner side has an armchair pattern; the preoptimized geometry is obtained by rotating the central hexagonal hole 30 degrees against the outer side. This kind of TCNT is called an inner-rim rotated case as discussed in the text. This molecule corresponds to indices (4, 6, 3, 3).

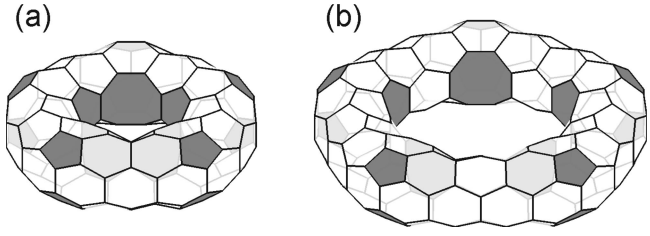

Figure 5. Two D_{5h} TCNTs with 5 octagons at the equators. Their indices are (2, 0, 1, 1) and (2, 0, 1, 2), respectively.

heptagons to the inner-rim regions, we can obtain the following simple criteria for stability:

$$\frac{n_{77}/2}{n_{77}+2n_{75}+n_{55}} < \frac{1}{4} \text{ and } \frac{n_{77}/2+n_{75}}{n_{77}+2n_{75}+n_{55}} > \frac{1}{4} \qquad (6)$$

which can be further simplified as $|n_{55}-n_{77}| < 2n_{75}$.

As mentioned by Berger et al., the value of n_{rot} that minimizes the cohesive energy of TCNTs depends on the choice of index set. Our preliminary geometry optimization based on the potential energy function proposed by Lenosky et al.[32] shows that cohesive energies for TCNTs with $n_{rot} =$ 5, 6, or even 7 are lower than those with other values of rotational symmetry number. Using our construction scheme and the Lenosky's potential, we found that there are about ten stable small TCNTs with the total number of carbon atoms less than 100 and about several hundred TCNTs with less than 500 carbon atoms.

Special Cases: Quadrilateral and Octagon. One should notice that for TCNTs belonging to the D_{nh} point group, if we set $n_{77}(n_{55}) = 0$, n_{rot} pairs of heptagons (pentagons) will merge at the equator to form n_{rot} octagons (quadrilaterals). In agreement with Ihara et al.,[33] the geometry optimization indicates that the existence of an 8-member ring is much more energetically favored than that of a 4-member ring. Thus, D_{nh} TCNTs or end-capped double-wall CNTs[5,31] containing pentagons and octagons might be a reasonable possibility to be examined in a further study. Figure 5 shows the two smallest 5-fold TCNTs with pentagons and octagons.

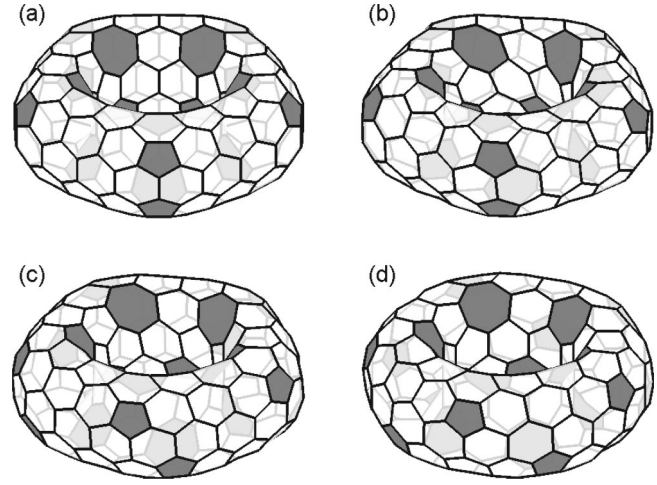

Figure 6. (a) D_{5h} parent TCNT with indices (2, 1, 1, 2). (b) Derived TCNT from the structure in (a) with the inner-rim shifted by one unit ($is = 1$). Heptagons in the inner-rim are rearranged in the staggered conformation. (c) Derived TCNT from the structure in (b) by applying a further shifting on the outer-rim by one unit but in the opposite direction ($is = 1$, $os = -1$). Note that this "anti-shifting" on the outer side releases part of the strain energy caused by the inner-rim shift, as can be seen from the degree of distortion especially in the inner-rim as compared to (b). (d) Derived TCNT from the structure in (c) by applying one more outer-rim shifting ($is = 1$, $os = -2$). This TCNT has D_{5d} symmetry, and the strain energy is further released.

ISOMERIZATIONS OF TCNTS

Horizontal Shifting: D_{nd} Isomers. In a previous section, we have shown how a chiral TCNT with D_n symmetry can be constructed from a hollowed prism. Alternatively, it is also possible to perform a suitable isomerization to generate a TCNT with only D_n symmetry from an achiral D_{nh} parent TCNT (see Figure 6(a)). For instance, in Figure 6(b), we have a distorted TCNT derived from the parent TCNT in Figure 6(a) by an *inner-shift*, which will be denoted as *is*. The heptagons in the inner-rim of the transformed TCNT are shifted in such a way that heptagons in the upper and the lower parts of the torus are rearranged in the staggered conformation instead of in the eclipsed conformation as in the original parent molecule. We can see clearly that the inner-rim of TCNT in Figure 6(b) is highly strained due to the horizontal shift. Interestingly, the strain energy accumulated inside can be partly released by performing an additional *outer-shift* transformation in the opposite direction operating on the outer-rim as shown in Figure 6(c). We denote this additional operation by $os = -1$. It is interesting to note that both of these two transformed isomers are chiral TCNTs. A further reduction of strain energy can be achieved by one more outer-shift transformation on the TCNT in Figure 6(c). By inspection, the resulting TCNT in Figure 6(d), which belongs to the D_{5d} point group, has an arrangement of the pentagons and heptagons in the symmetrical staggered conformation.

There are many theoretically proposed D_{nd} TCNTs in the literature. Many of them are expected to be thermally stable.[20,21,24,25,34,35,37] With carefully chosen parities of the four indices and the size of horizontal shifting described above, we can obtain TCNTs with D_{nd} symmetry as shown in Figure 7. Incidentally, a D_{nd} TCNT can also be viewed as a *hollow-antiprism*, as compared to the D_{nh} hollow-prism case. Thus, starting from a set of four indices (n_{75}, n_{77}, n_{55}, s),

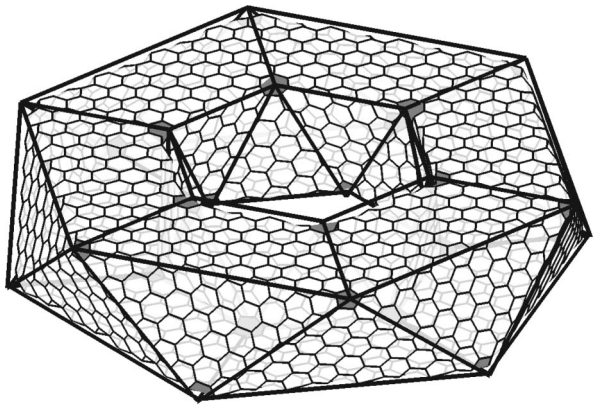

Figure 7. The antiprism isomer of $(n_{75}, n_{77}, n_{55}, s) = (2, 1, 1, 2)$, $(n_1, n_2) = (2, 1)$ and $n_{rot} = 6$. The nonhexagons still are located at the vertices of the polyhedron, but pentagons and heptagons are in a staggered conformation compared to the eclipsed conformation of the hollow-prism TCNT.

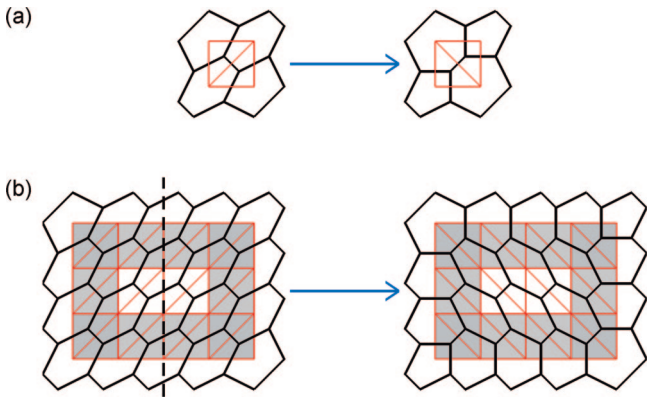

Figure 8. The definition of a Stone-Wales transformation (a) and its generalized form (b). Equilateral triangles with red edges are the dual graph of the graphene lattice, so each triangle corresponds to a trivalent carbon atom. The generalized SWT is formally equivalent to performing a reflection on the rectangular patch of the dual graph of graphite (dashed lines). Only the connectivities of the atoms within the shaded region are affected by the generalized SWT.

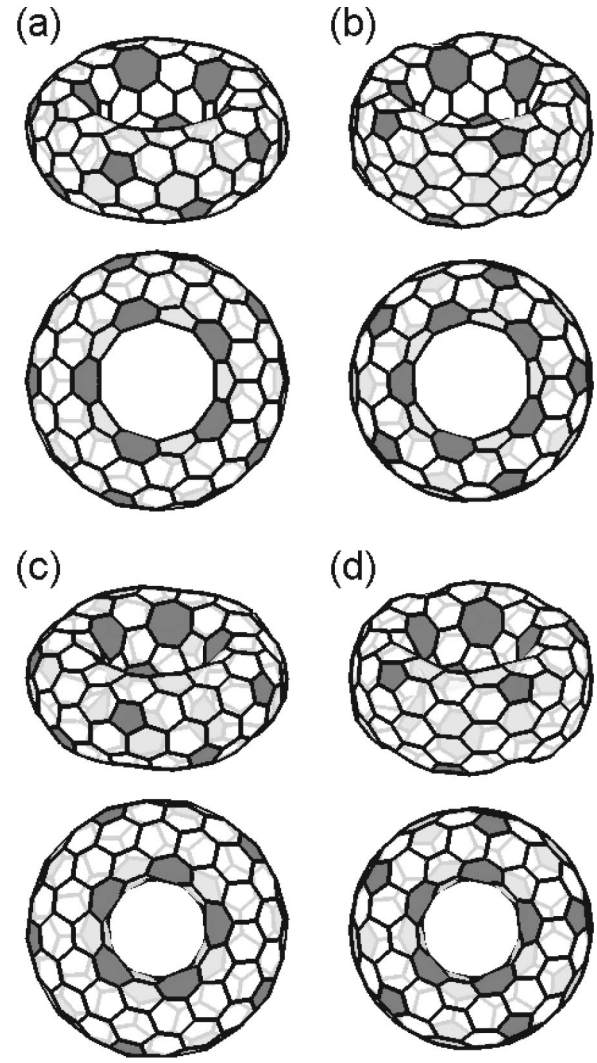

Figure 9. Four derived D_{5d} isomers by applying the generalized SWT to a parent D_{5d} TCNT with 240 atoms and the indices, (2, 1, 1, 2). This set of indices corresponds to type 1 TCNTs listed in Table 1.

we can generate a whole series of isomers through the horizontal shifting. In general, there is one pair of stable D_{nd} and D_{nh} isomers, and there are numerous D_n chiral intermediates ranging in between these two high-symmetry structures.

Generalized Stone-Wales Transformation: Induced Chirality and Edge Transformation. Fowler et al.[29] proposed a D_5 chiral TCNT derived by five concerted Stone-Wales transformations (SWT)[28] of pentagon pairs from a D_{5d} parent TCNT that contains 120 carbon atoms (see Figure 8(a)). The SWT changes only the connectivity of the central two carbon atoms; it does not change the configuration of the rest of atoms in the molecule. Here, we generalize this transformation to an isomerization that includes all atoms within the graphene sheet specified by the parallelogram as shown in Figure 8(b). The effect of the generalized SWT on the local connectivity of a graphene lattice can be visualized easier by its dual graph. As can be seen from the Figure 8(b), only carbon atoms within the rectangular patch defined by two diagonal pentagons are influenced by the generalized SWT. Note that the vertices of the dual graph at the upper-left and the lower-right corners of the parallelogram have their vertex degrees increased by one, and the rest have two corners of their vertex degrees decreased by one. Thus, the two pentagons at the upper-left and the lower-right corners and two hexagons at the other two corners switch their locations after a generalized SWT. A similar generalized SWT can also be introduced for the situation where the pentagons are replaced by heptagons. In general, the two nonhexagons located at the corner of a diagonal switch their positions with the two hexagons on the other diagonal under the generalized SWT.

For an achiral D_{nd} TCNT with $n_{55}n_{77} \neq 0$, and some particular parities of indices, $(n_{75}, n_{77}, n_{55}, s)$, there exist four distinct transformed isomers that preserve the D_{nd} symmetry (see Figure 9). In Figure 9(a),(b), we show the structures of the parent D_{5d} TCNT and the transformed TCNT with only the pentagons distributed in the outer-rim transformed. Note that the outer perimeter of the transformed structure now has an armchair pattern which can be seen clearly in the bird view, and while seen from the top view, heptagons and pentagons are located in the staggered conformation. In Figure 9(c), we show the structure of another isomer with heptagons in the inner-rim transformed instead. In this case, the outer perimeter has a zigzag pattern, while the inner perimeter becomes an armchair pattern. And finally in Figure 9(d) we show the TCNT which has both of its inner- and

Table 1. Classification of the D_{nd} Tori Derived from the Generalized SWT Based on the Parity of Indices (n_{75}, $2n_{77}$, $2n_{55}$, s)[a]

type	(n_{75}, $2n_{77}$, $2n_{55}$, s)	SWT7	SWT5	minimal index value	number of atoms per unit cell
1	(*e*,*e*,*e*,*e*)	off	off	(2,0,0,2)	24
		off	on	(2,0,2,2)	40
		on	off	(2,2,0,2)	32
		on	on	(2,2,2,2)	48
2	(*o*,*o*,*e*,*o*)	off	off	(1,1,0,1)	8
		off	on	(1,1,2,1)	16
3	(*o*,*e*,*o*,*e*)	off	off	(1,0,1,2)	16
		on	off	(1,2,1,2)	24
4	(*e*,*e*,*o*,*e*)	off	on	(2,0,1,2)	32
		on	on	(2,2,1,2)	40
5	(*e*,*o*,*e*,*e*)	on	off	(2,1,0,2)	28
		on	on	(2,1,2,2)	44
6	(*e*, *o*, *o*, *o*)	off	off	(2,1,1,1)	24
7	(*o*, *o*, *o*, *o*)	off	on	(1,1,1,1)	12
8	(*o*, *o*, *o*, *e*)	on	off	(1,1,1,2)	20
9	(*e*, *o*, *o*, *e*)	on	on	(2,1,1,2)	36

[a] We used the alphabet *e* and *o* to denote parity even and parity odd for these four parameters. Since n_{77} and n_{55} is doubled so *e* is for integers and *o* for half-integers. In some of these different situations, we can apply a further generalized SWT to heptagons in the inner-rim (SWT7) or pentagons in the outer-rim (SWT5). We denote the situation that the generalized SWT can be applied by "on" and otherwise by "off". For example, D_{nd} TCNT of type 1 is characterized by even n_{75} and s and integral values for n_{77} and n_{55}. In this case, both SWT5 and SWT7 can be freely imposed on the parent TCNT; therefore, if $n_{77}n_{55} \neq 0$, there are four distinct isomers, see Figure 9 for their structures. Readers of interest may reach to the Supporting Information for the optimized geometries for all nine types and sixteen cases listed.

outer-rims transformed by the generalized SWT. Not surprisingly, both the inner- and outer-rims of this TCNT exhibit armchair patterns. If we view this molecule from the top, heptagons in the inner-rim and pentagons in the outer-rim are arranged in the eclipsed conformation, which is similar to the original parent molecule as shown in Figure 9(a).

It should be noted that the generalized SWT described here is exactly the D_{nd} version of the inner- or outer-rim rotation discussed in the previous section, where we have shown a D_{6h} example in Figure 4. It can be said that the generalized SWT is an alternative perspective of inner- and outer-rim rotation in the D_{nd} TCNT case. However this is not true for D_{nh} TCNTs because the rotation essentially changes the number of atoms in this case, while generalized SWT, which is an isomerization process, does not. This rather complicated issue will be addressed in more detail in a subsequent report.

Small symmetric TCNTs that can be derived from the generalized SWT are of particular interest. In Table 1 we list all possible small D_{nd} TCNTs in this scheme, which can be further classified into 9 types and 16 different index parities, with *e* and *o* standing for *even* and *odd* of the corresponding index. The n_{rot} concerted generalized SWTs performed on the outer-rim pentagon pairs are denoted as SWT5, while the generalized SWTs on the inner-rim heptagon pairs are denoted as SWT7. Readers interested in the detailed structures listed in the table may refer to the Supporting Information of this paper, where the AM1-optimized geometries of the TCNTs are charted for each case. Itoh et al. probably were the first to propose many of these structures listed in the table.[25] In their notation, a *b*-located pentagon corresponds to our SWT5 structures, and a *c*-located heptagon corresponds to the SWT7 structures. It is emphasized here that only in the D_{nd} TCNT case are these four different structures the result of a general isomerization process and can be described succinctly by the generalized SWT. However, the generalized SWT cannot be applied to the TCNTs belonging to the D_{nh} point group; therefore, there are no isomers that can be derived from this kind of parent molecule through the SWT.

Finally, we want to emphasize that the two kinds of isomerizations introduced in this section, the horizontal shifting and the generalized SWT, can be applied not only to the achiral TCNTs with chiral vectors, (1, 0) or (1, 1), but also to other chiral TCNTs with different chiral vectors as well.

HELICAL CARBON NANOTUBES

As mentioned above and shown in Figure 6, the two chiral TCNTs generally have much higher strain energy than those with D_{nd} or D_{nh} symmetry. Here we show another way to release this extra strain is by dissecting the TCNT along any of its longitudes. The more distorted the original TCNT parent molecule is, the more helicity the derived HCNT will have. In Figure 10(b),(c), we show two transformed TCNTs derived from the parent D_{5h} TCNT (Figure 10(a)) by the different outer-shifting operations. As discussed in the previous section, the TCNT in Figure 10(b) is the transformed structure with $os = 1$. If we dissect this structure along a certain longitude, we can obtain a helical structure with the optimized geometry as shown in Figure 10(d). Following the arrow to the right as shown in Figure 10, we have the TCNT with $os = 2$ (Figure 10(c)). It is clear that the excess strain energy in this molecule is larger than that of the TCNT with $os = 1$ due to the larger distortion introduced by the out-shifting transformation; therefore, the resulting optimized HCNT has a larger pitch angle, as expected. Similarly, another family of HCNTs can be generated by performing inner-rim shifts first and then dissecting the distorted TCNT along any of its longitudes.

Our preliminary calculation on the three-dimensional structures of these HCNTs by using the simple Lenosky's potential[32] indicates that the pitch angle is roughly related to the indices of the parent TCNT and the shifting parameters, *is* and *os*, by

$$\tan\theta \propto \frac{is}{(n_{77}+n_{55}+2n_{75})s} \propto \frac{os}{(n_{77}+n_{55}+2n_{75})(s+n_{75})} \tag{7}$$

Further studies on the relaxed geometric structures of HCNTs for different shifting parameters classified in this scheme based on the quantum chemical calculations would be interesting and are currently underway in our research group.

CORRESPONDENCE TO EXISTING CLASSIFICATION SCHEMES

In this section, we show the relationships between our classification method and other existing schemes. First of all, we consider the classification and construction scheme proposed by Akagi et al.[30,35] Their method is based on specifying eight parameters, which are four vectors on a hexagonal honeycomb lattice. When the vectors, *a* and *b*, are parallel to the armchair and zigzag lines of graphene,

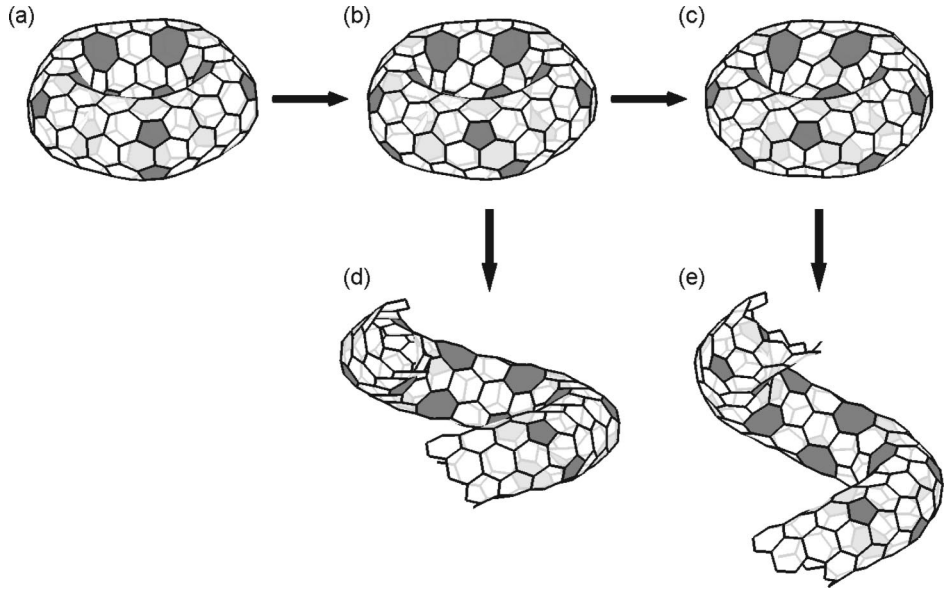

Figure 10. A distorted TCNT can release its additional strain by cutting out the bonds on a certain longitude and recoils to form a HCNT. The magnitude of helicity depends on how the parent TCNT is distorted. (a) Parent TCNT with D_{5h} symmetry; transformed isomers with (b) $os = -1$ and (c) $os = -2$, respectively; HCNTs in (d) and (e) are the derived HCNTs from TCNTs in (b) and (c) by dissection, respectively.

respectively, i.e. the type I classification, with $M_y = 0$, so the axial vector of the HCNT, $\vec{M}$, is parallel to the zigzag or armchair direction of the honeycomb lattice, we would have

$$\begin{gathered} n_{75} = a \\ n_{77} = b \\ n_{55} = |L_y - 2(a+b)| \\ s = M_x - a \\ (n_1, n_2) = (1, 0) \\ os = L_x \end{gathered} \tag{8}$$

When $L_y - 2(a+b)$ is negative, a generalized SWT that involves pentagons is needed. The type II then corresponds to $(n_1, n_2) = (1, 1)$. However, if $M_y \neq 0$, then an additional twisting must be made perpendicular to the tube axis.

Starting from a planar tiling of rows of heptagons and pentagons, with certain hexagon rows inserted in between, László et al.[37] obtained the connectivity of a D_{nd} TCNT by selecting a suitable super cell and applying a periodic boundary condition. The TCNTs thus derived are also special cases of the scheme proposed in the present paper, with indices listed below:

$$\begin{gathered} n_{75} = l \\ n_{77} = 1 \\ n_{55} = \begin{cases} 1 & l \text{ is even} \\ 0 & l \text{ is odd} \end{cases} \\ s = 1 \\ (n_1, n_2) = (1, 0) \end{gathered} \tag{9}$$

If the super cell lattice vectors chosen are not parallel to the basis vector of the tiling, the resulting connectivity will lead to a HCNT. For example, if $\vec{b}_1 = \vec{a}_1 - \vec{a}_2$ and $\vec{b}_2 = N(\vec{a}_1 + \vec{a}_2)$, where N is the number of unit cells, then the HCNT is corresponding to $(n_{75}, n_{77}, n_{55}, s, n_1, n_2)$ given above and with $is = s$ or $os = n_{75} + s$, with respect to D_{nd} conformation. And if $\vec{b}_1 = \vec{a}_1 - 2\vec{a}_2$ is chosen instead, the corresponding shifting parameter in our scheme is $is = 2s$ or $os = 2(n_{75}+s)$.

The relationship between our classification scheme and the systematic construction rule for a family of D_{nd} TCNTs using the triangular tiling on a rectangular plane by a set of the four indices (m, g_1, g_m, z) developed by Berger and Avron[20,21] has also been worked out. Here we provide the indices correspondence

$$\begin{aligned} n_{75} &= (g - g_1 - g_m)/2 \\ &\quad \text{where } g = g_1 + g_{mid} + g_{end} + g_m \\ &\quad g_{mid} = \begin{cases} 0 & m = 2 \\ z & 3 \le m < 5 \\ 2^{\lfloor (m+1)/2 \rfloor - 3} z & \text{otherwise} \end{cases} \\ &\quad g_{end} = \begin{cases} 2^{\lfloor (m+1)/2 \rfloor - 1} z & m \text{ is even and } m \ge 4 \\ 0 & \text{otherwise} \end{cases} \\ n_{77} &= |g_1 - z| \\ n_{55} &= \begin{cases} |2^{m/2-1} z - g_m| & m \text{ is even} \\ g_m & \text{otherwise} \end{cases} \\ s &= \begin{cases} z & g_1 < z < g_1 + g_m \text{or } m \ge 3 \\ 2z - g_1 & \text{otherwise} \end{cases} \\ \text{SWT7} &= \begin{cases} 1 & g_1 - z < 0 \\ 0 & \text{otherwise} \end{cases} \\ \text{SWT5} &= \begin{cases} 1 & m \text{ is even and } 2^{m/2-1} z - g_m < 0 \\ 0 & \text{otherwise} \end{cases} \end{aligned} \tag{10}$$

If $m = 2$ and $z \ge g_1 + g_m$, the number of atoms in the outer rim equals the number of atoms in the inner rim ($n_{75} = 0$), which is considered to be quite unstable.

CONCLUSION

In summary, starting from the hollow-prism construction of D_{nh} TCNTs proposed by Tamura et al., we have developed a generalized classification scheme for a larger class of highly symmetric TCNTs, which can be characterized by a certain number of geometric parameters. By means of shifting between latitudinal polyacetylene chains of a parent D_{nh}

TCNT, a series of distorted D_n-symmetric isomers can be realized, and dissecting them longitudinally leads to the corresponding HCNTs of various helicities, depending on the prescribed shifting parameters. In particular, a subset of these isomers with D_{nd} symmetry together with the derivatives generated by the generalized Stone-Wales transformation nearly includes all possible TCNTs using the construction methods and individual cases of TCNTs in the literature as special cases of our general method. Preliminary quantum chemical calculations show that a large number of TCNTs in this scheme may have cohesive energies lower than C_{60}, which shall be discussed in our following reports.

ACKNOWLEDGMENT

We wish to acknowledge the financial support of NSC, Taiwan, ROC. B.-Y. Jin wishes to acknowledge the useful support from the Center of Quantum Science and Engineering, NTU, Taiwan.

Supporting Information Available: Detailed structures of the AM1-optimized geometries for these smallest D_{nd} TCNTs with *ncell* = 5 for each group as specified in Table 1. This material is available free of charge via the Internet at http://pubs.acs.org.

REFERENCES AND NOTES

(1) Kroto, W.; Heath, J.; O'Brien, S.; Curl, R.; Smalley, R. C_{60} Buckministerfullerene. *Nature* **1985**, *318*, 162–163.
(2) Iijima, S. Helical microtubules of graphitic carbon. *Nature* **1991**, *354*, 56–58.
(3) Saito, R.; Dresselhaus, G.; Dresselhaus, M. In *Physical Properties of Carbon Nanotubes*, 1st ed.; World Scientific Publishing Company: Singapore, 1998; pp 35−58.
(4) Krishnan, A.; Dujardin, E.; Treacy, M.; Hugdahl, J.; Lynum, S.; Ebbesen, T. Graphitic cones and the nucleation of curved carbon surfaces. *Nature* **1997**, *388*, 451–454.
(5) Iijima, S.; Ichihashi, T.; Ando, Y. Pentagons, heptagons and negative curvature in graphite microtubule growth. *Nature* **1992**, *356*, 776–778.
(6) Hashimoto, A.; Suenaga, K.; Gloter, A.; Urita, K.; Iijima, S. Direct evidence for atomic defects in graphene layers. *Nature* **2004**, *430*, 870–873.
(7) Zhang, X.; Zhang, Z. Polygonal spiral of coil-shaped carbon nanotubes. *Phys. Rev. B* **1995**, *52*, 5313–5317.
(8) Sarkar, A.; Kroto, H.; Endo, M. Hemi-toroidal networks in pyrolytic carbon nanotubes. *Carbon* **1995**, *33*, 51–55.
(9) Suenaga, K.; Wakabayashi, H.; Koshino, M.; Sato, Y.; Urita, K.; Iijima, S. Imaging active topological defects in carbon nanotubes. *Nat. Nanotech.* **2007**, *2*, 358–360.
(10) Tamura, R.; Tsukada, M. Disclinations of monolayer graphite and their electronic states. *Phys. Rev. B* **1994**, *49*, 7697–7708.
(11) Ahlskoga, M.; Seynaevea, E.; Vullersa, R.; Van Haesendoncka, C.; Fonsecab, A.; Hernadib, K.; Nagy, J. Ring formations from catalytically synthesized carbon nanotubes. *Chem. Phys. Lett.* **1999**, *300*, 202–206.
(12) Tamura, R.; Ikuta, M.; Hirahara, T.; Tsukada, M. Positive magnetic susceptibility in polygonal nanotube tori. *Phys. Rev. B* **2005**, *71*, 045418.
(13) Tsai, C.; Shyu, F.; Chiu, C.; Chang, C.; Chen, R.; Lin, M. Magnetization of armchair carbon tori. *Phys. Rev. B* **2004**, *70*, 075411.
(14) Liu, L.; Guo, G.; Jayanthi, C.; Wu, S. Colossal paramagnetic moments in metallic carbon nanotori. *Phys. Rev. Lett.* **2002**, *88*, 217206.
(15) Latil, S.; Roche, S.; Rubio, A. Persistent currents in carbon nanotube based rings. *Phys. Rev. B* **2003**, *67*, 165420.
(16) Shyu, F. Magneto-optical properties of carbon toroids. Influence of geometry and magnetic field. *Phys. Rev. B* **2005**, *72*, 045424.
(17) Rocha, C.; Pacheco, M.; Barticevic, Z.; Latge, A. Carbon nanotube tori under external fields. *Phys. Rev. B* **2004**, *70*, 233402.
(18) Sasaki, K. Vacuum structure of toroidal carbon nanotubes. *Phys. Rev. B* **2002**, *65*, 155429.
(19) Lin, M. Magnetic properties of toroidal carbon nanotubes. *J. Phys. Soc. Jpn.* **1998**, *67*, 1094–1097.
(20) Avron, J.; Berger, J. Tiling rules for toroidal molecules. *Phys. Rev. A* **1995**, *51*, 1146–1149.
(21) Berger, J.; Avron, J. Classification scheme for toroidal molecules. *J. Chem. Soc., Faraday Trans.* **1995**, *91*, 4037–4045.
(22) Itoh, S.; Ihara, S.; Kitakami, J. Toroidal form of carbon C_{360}. *Phys. Rev. B* **1993**, *47*, 1703–1704.
(23) Ihara, S.; Itoh, S.; Kitakami, J. Toroidal forms of graphitic carbon. *Phys. Rev. B* **1993**, *47*, 12908–12911.
(24) Itoh, S.; Ihara, S. Toroidal forms of graphitic carbon. II. Elongated tori. *Phys. Rev. B* **1993**, *48*, 8323–8328.
(25) Itoh, S.; Ihara, S. Isomers of the toroidal forms of graphitic carbon. *Phys. Rev. B* **1994**, *49*, 13970–13974.
(26) Setton, R. Toroidal structures and limits of a model for the construction of helical and s-shaped nanotubes. *Carbon* **1997**, *35*, 497–505.
(27) Dunlap, B. Connecting carbon tubules. *Phys. Rev. B* **1992**, *46*, 1933–1936.
(28) Stone, A.; Wales, D. Theoretical studies of icosahedral C_{60} and some related species. *Chem. Phys. Lett.* **1986**, *128*, 501–503.
(29) Ceulemans, A.; Chibotaru, L.; Fowler, P. Molecular anapole moments. *Phys. Rev. Lett.* **1998**, *80*, 1861–1864.
(30) Akagi, K.; Tamura, R.; Tsukada, M.; Itoh, S.; Ihara, S. Electronic structure of helically coiled carbon nanotubes: relation between the phason lines and energy band features. *Phys. Rev. B* **1996**, *53*, 2114–2120.
(31) Iijima, S.; Ajayan, P.; Ichihashi, T. Growth model for carbon nanotubes. *Phys. Rev. Lett.* **1992**, *69*, 3100–3103.
(32) Lenosky, T.; Gonze, X.; Teter, M.; Elser, V. Energetics of negatively curved graphitic carbon. *Nature* **1992**, *355*, 333–335.
(33) Ihara, S.; Itoh, S.; Akagi, K.; Tamura, R.; Tsukada, M. Structure of polygonal defects in graphitic carbon sheets. *Phys. Rev. B* **1996**, *54*, 14713–14719.
(34) Oh, D.; Park, J.; Kim, K. Structures and electronic properties of small carbon nanotube tori. *Phys. Rev. B* **2000**, *62*, 1600–1603.
(35) Dunlap, B. Constraints on small graphitic helices. *Phys. Rev. B* **1994**, *50*, 8134–8137.
(36) Goldberg, M. A class of multi-symmetric polyhedra. *Tohoku Math. J.* **1937**, *43*, 104–108.
(37) László, I.; Rassat, A. The geometric structure of deformed nanotubes and the topological coordinates. *J. Chem. Inf. Comput. Sci.* **2003**, *43*, 519–524.

CI800395R